energies

MDPI

Article

Integration of a Heterogeneous Battery Energy Storage System into the Puducherry Smart Grid with Time-Varying Loads

M A Sasi Bhushan [1], M. Sudhakaran [1], Sattianadan Dasarathan [2,*] and Mariappane E [3]

[1] Department of EEE, Puducherry Technological University, Puducherry 605014, Puducherry, India; masasibhushan@ptuniv.edu.in (M.A.S.B.); sudhakaran@ptuniv.edu.in (M.S.)
[2] Department of EEE, Faculty of Engineering & Technology, SRM Institute of Science and Technology, Kattankulathur 603203, Tamilnadu, India
[3] Department of ECE, Christ Institute of Technology, Villianur Commune, Puducherry 605502, Puducherry, India; dev_mari@rediffmail.com
* Correspondence: sattiand@srmist.edu.in

Abstract: A peak shaving approach in selected industrial loads helps minimize power usage during high demand hours, decreasing total energy expenses while improving grid stability. A battery energy storage system (BESS) can reduce peak electricity demand in distribution networks. Quasi-dynamic load flow analysis (QLFA) accurately assesses the maximum loading conditions in distribution networks by considering factors such as load profiles, system topology, and network constraints. Achieving maximum peak shaving requires optimizing battery charging and discharging cycles based on real-time energy generation and consumption patterns. Seamless integration of battery storage with solar photovoltaic (PV) systems and industrial processes is essential for effective peak shaving strategies. This paper proposes a model predictive control (MPC) scheme that can effectively perform peak shaving of the total industrial load. Adopting an MPC-based algorithm design framework enables the development of an effective control strategy for complex systems. The proposed MPC methodology was implemented and tested on the Indian Utility 29 Node Distribution Network (IU29NDN) using the DIgSILENT Power Factory environment. Additionally, the analysis encompasses technical and economic results derived from a simulated storage operation and, taking Puducherry State Electricity Department tariff details, provides significant insights into the application of this method.

Keywords: quasi-dynamic load flow analysis; distributed energy resources; PV-BESS; state of charge; peak shaving; model predictive control; economic analysis

Academic Editor: JongHoon Kim

Received: 26 November 2024
Revised: 10 January 2025
Accepted: 11 January 2025
Published: 19 January 2025

Citation: Sasi Bhushan, M.A.; Sudhakaran, M.; Dasarathan, S.; E, M. Integration of a Heterogeneous Battery Energy Storage System into the Puducherry Smart Grid with Time-Varying Loads. *Energies* **2025**, *18*, 428. https://doi.org/10.3390/en18020428

1. Introduction

Distribution networks exhibit high energy losses and low voltage stability due to their high current and low voltage levels. Integrating distributed energy resources (DERs) has become a significant area in distribution power system research, offering advantages such as reducing network power losses and improving voltage profiles and system reliability. Improper integration of DERs may lead to technical, economic, and safety-related issues. DERs, such as PV units, have stochastic output power constraints, posing challenges to reliable power system operation [1].

BESSs offer a promising solution to enhance system flexibility and address the intermittency of DERs. These systems can be modeled using various methods, including circuit models, which are particularly suitable for dynamic simulations. BESSs are valuable for providing ancillary grid services, improving distribution network performance and

participating in demand response programs by adjusting energy usage during peak times to avoid expensive infrastructure upgrades [2].

Integrating BESSs with a PV system increases energy availability and boosts PV penetration in distribution networks, though sizing and placement pose complex optimization challenges. Efficient battery management systems (BMSs) are crucial for minimizing energy losses and prolonging battery life through intelligent charging algorithms [3].

High peak electricity demand leads to increased costs for utilities and consumers. BESSs, particularly those using electrochemical technology, are effective in peak shaving by charging during off-peak times and discharging during peak demand. While large-scale BESS deployment presents operational challenges, these systems are economically viable when optimized for capacity and demand profiles, significantly enhancing energy efficiency and reducing peak demand in both internal microgrids and external networks [4].

Summary of Previous Work

Using a mixed-integer linear programming model, the authors of [5] proposed a planning-operation-based methodology to address the location and size selection problem of BESSs and renewable distributed generators (DGs). In [6], a two-layer optimization structure was created for optimal use of BESSs and renewable energy sources. The multi-objective optimization problem for a 33-bus test distribution network was solved using moth search optimization. An optimization process [7,8] was applied using the newly introduced Coyote Optimization Algorithm to simulate four scenarios involving various PV and BESS conditions. Time-varying voltage-dependent load models were proposed to determine the penetration level of photovoltaic units in a distribution network [9]. Different load models resulted in varying levels of penetration after PV allocation. The authors of [10] proposed a mixed-integer quadratic programming model with quadratic constraints to determine the optimal number, sitting, and sizing of multiple types of DG units for power loss minimization. In [11], mixed-integer optimization using a Genetic Algorithm was presented to determine the optimal size and location of Battery-Sourced Distributed Photovoltaic Generation (B-SDPVG) in distribution networks. In the referenced paper, the Total Energy Loss Index was formulated as the primary objective function, while bus voltage deviations and B-SDPVG penetration levels were simultaneously calculated. To determine the optimal contract capacities and sizes of battery energy storage systems (BESSs) for time-of-use rate customers, advanced multi-pass dynamic programming and expert knowledge base rules were applied [12]. A methodology was developed for distribution engineers to evaluate the required amount of distributed energy storage (DES) for different transmission and/or distribution capacities. The primary focus of this work was on technical design and operations, with financial aspects and specific modular energy storage technologies receiving only incidental attention and a solution for BESS dimensioning and implementing a novel control algorithm with adjustable state-of-charge limits and the application of emergency resistors. A stochastic-based BESS planning method was developed to determine the optimal sizing and location of BESS, aiming to minimize total investment and operational costs while considering energy savings achieved through conservation voltage reduction [13].

A bi-level optimization model was created to identify the best placement and sizing of a battery energy storage system within a distribution network. This model aims to minimize the total net present value (NPV) of the network throughout the project's life cycle. In the referenced work, a newly modified particle swarm optimization technique was used to determine the optimal configuration of the distribution network [14,15].

Control algorithms and pricing or incentive schemes for peak shaving, are often in conjunction with other objectives, such as maximizing the self-consumption of solar PV.

In [16], a simple dispatch strategy for residential peak shaving using building-based energy storage was proposed, and the economics of various storage technologies operating under a Con Edison demand tariff were investigated. In [17], the effects of storage and solar PV curtailment on peak shaving were investigated, showing that curtailment can specifically reduce peak PV export by half with less than a 7% annual reduction in self-consumption. The authors also considered the real-time optimization of DNO-owned storage for peak reduction, developing storage controllers that incorporate demand forecasts and consumer clustering. The flexibility offered by the electrification of heating and cooling has been considered, where electric power was stored as thermal energy. A DSM algorithm was proposed to smooth the load curve and achieve non-disruptive peak shaving [18].

The literature on using BESSs for peak load shaving [19–22] primarily addresses two key issues: the control method for BESS operation and the system architecture for real-world implementation. BESS operations are typically optimized based on load forecasts, and the effectiveness of peak load shaving is also evaluated. Personalized pricing strategies encourage demand management and minimize system demand peaks by offering consumers tailored non-discriminatory price tariffs. In [23,24], an examination of the economic viability of electrochemical storage systems, such as batteries and flow batteries, in response to time-of-use tariffs in Italy, which focused on public institutions, demonstrated through case studies that the current costs of battery storage systems make them economically feasible only when there is a substantial difference between peak and off-peak electricity prices.

An effective cost model is crucial to evaluate economic feasibility and determine optimal construction scale and material selection. A life cycle cost model for energy storage systems was introduced in [25], comparing and analyzing various systems using the annualized storage life cycle cost and the levelized cost. In [26], the researchers introduced a groundbreaking life cycle cost model for recycling lithium-ion batteries from electric vehicles, highlighting both financial aspects and sustainability. The study conducts a comparative analysis across three techno-economic scenarios, focusing on various stakeholders. Building on the established life cycle cost model [27], a sizing method with sensitivity analysis for battery–supercapacitor hybrid energy storage systems was proposed. This method examines the impact of various factors on the overall system cost. Based on existing cost models, numerous studies have been conducted on energy storage materials and scale design [28]. In [29], a bi-level model for the optimal location and scale of grid-side battery energy storage systems was proposed, featuring coordinated planning and operation, effectively reducing operational costs and losses.

The study optimized the management of a lithium-ion-based BESSs to maximize electricity bill savings from peak shaving while minimizing battery degradation [30]. The focus was on modeling battery degradation mechanisms and assessing the economic benefits rather than the impact on the distribution grid. In [31], a large-scale profitability analysis for peak shaving was conducted using over 5300 industrial customer load profiles in Germany. In [32–34], the authors concluded that peak shaving technology offers the highest profits compared to other battery use cases. They also stated that minimal payback periods for peak shaving operations can be achieved in many instances.

In [35], the study of a BESS located within a distribution grid was optimized to determine the optimal size, location, and control strategy. Based on a 20 kV distribution grid in Kabul with 22 buses, the research concluded that an optimally placed BESS utilizing a peak shaving strategy can significantly enhance system performance, reducing power losses by up to 20.62%. Significant energy savings can be achieved through the scheduling of industrial loads. Many researchers have suggested in their future recommendations that integrating renewable sources with DSM is feasible for both commercial and industrial

sectors. To implement demand-side management, large-scale building loads (industrial loads) are scheduled to minimize energy consumption during peak hours and reduce overall energy costs. Additionally, powering the system with renewable energy sources is proposed to enhance environmental sustainability.

This paper exhibits the implementation of peak load shaving for Indian practical distribution, including the following objectives:

(i) Integration of a PV system with a battery energy storage system for industrial loads
(ii) Proposing MPC-based optimized control to find the optimal PV-BESS
(iii) Adopting the reliable PV-BESS model for peak shaving application
(iv) Proposing the economic analysis for PV-BESS installation.

This paper is organized as follows: Sections 2 and 3 of the article describe the investigation of PV-BESS integration and peak shaving in loads. Section 4 gives details of the peak shaving on the test system, BESS optimal control, strategy, and economic benefits of BESSs. Then, the findings and conclusions of the study are discussed in Section 5.

2. PV-BESS Integration

Integrating PV systems and BESSs for industrial peak shaving involves several technical, operational, and regulatory constraints. Figure 1 depicts a typical block diagram of a distribution network with PV-BESS integration.

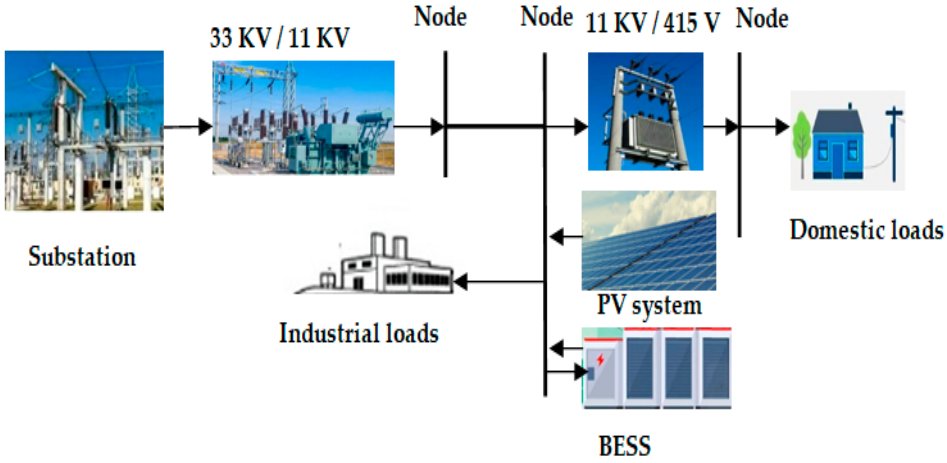

Figure 1. Block diagram of a distribution network with PV-BESS.

The primary technical restrictions are taken into account when developing the BESS model. Using the BESS round-trip efficiency $\eta_{RTP}(\alpha)$ at year α assumes identical charging and discharging efficiencies η_{Ch}&η_{Dis}, as in Equation (1):

$$\eta_{ch} = \eta_{Dis} = \sqrt{\eta_{RTP}(\alpha)} \quad (1)$$

The BESS power $P_{BESS}(t)$ is a combination of the discharging power $P_{Dis}(t)$ and the charging power $P_{Ch}(t)$

$$P_{BESS}(t) = P_{Ch}(t) - P_{Dis}(t) \quad (2)$$

However, the discharging action is indicated by the negative sign of $P_{Dis}(t)$ in Equation (2). The maximum of both charging and discharging power limitations, which are equivalent to the converter AC power rating, P_{nom}, limit both the charging and discharging powers, which are non-negative, presented in Equations (3) and (4).

$$0 \leq P_{ch}(t) \leq P_{nom} \quad (3)$$

$$0 \leq P_{Dis}(t) \leq P_{nom} \tag{4}$$

The optimization limitations are connected to the BESS's state of charge (SOC). The operating points of BESSs have a limited range of SOC to maintain battery discharge characteristics. The initial and final values of SOC should be the same in order to accurately reflect BESS capacity to optimize results expressed in Equation (5). It should be mentioned that the optimization data results will be used to determine the one-year operating profit of the defined systems.

$$SOC_{Min} \leq SOC(t) \leq SOC_{Max} \tag{5}$$

where SOC_{Min} and SOC_{Max} indicate the minimum and maximum permitted states of charge for a certain BESS system. In this study, the charging and discharging of the BESS are performed with SOC ranging in Equation (6) from 20% to 80%. During charging mode, SOC reaches 80%. However, in the battery's discharging mode, SOC decreases to 20%, and if there is little demand, electricity is used to charge the BESS until it reaches its maximum capacity of 80%.

$$SOC(t+1) = SOC(t) + \left(\eta_{Ch} \times P_{BESS}(t) - \frac{P_{BESS}(t)}{\eta_{Dis}}\right) \times \Delta t \tag{6}$$

where η_{Ch}&η_{Dis} represents the efficiency rates for the charging and discharging of the BESS; Δt represents the time step duration.

Battery capacity, an essential health metric, determines how well it will work during its entire life cycle, including the gradual deterioration of the battery's maximum capacity $C_\delta(t)$. SOC (7) at time t is then compared to the battery's complete capacity so that

$$SOC(t) = SOC(t-1) - \frac{1}{C_\delta(t)} \int_{t-1}^{t} I(\tau) d\tau. \tag{7}$$

The SOC change is calculated by dividing the current $I(\tau)$ between $t-1$ and t by the battery's entire capacity $C_\delta(t)$ at time t. C_{req} is the battery's minimum capacity; if $C_\delta(t)$ falls below C_{req}, the battery's life is over. T_l in Equation(8) stands for battery life, which is the amount of time needed for $C_\delta(t)$ to reach C_{req} such that

$$T_l = \min_t \{t | C_\delta(t) < C_{req}\} \tag{8}$$

In other words, T_l is the point in time at which deterioration causes the maximum battery capacity to fall below the necessary capacity. It is simple to estimate the cycle life if we know $C_\delta(t)$. The BESS is influenced by the charging pattern, which is typically illustrated through the battery cycle and depth of discharge (DOD). The DOD (t) describes how deeply the battery is discharged such that

$$DOD(t) = 1 - SOC(t) \tag{9}$$

As DOD declines, battery cycle life grows significantly. It is possible to accurately estimate the overall energy production over the battery's lifespan by analyzing DOD and cycle time. Planning a PV system begins with sizing BESS capacity for maximum profit, where the market structure plays an essential role in determining the appropriate BESS size for PV integration. If the penetration of renewable energy generators is low and the system marginal price (SMP) is constant, the financial benefits derived by BESSs will not be adequate to offset the system's total capital expenditures. However, as renewable energy source penetration increases and distribution system operators recognize the value of storage devices in reducing variability, a more significant gap between the maximum and minimum SMP enhances the profitability of a PV system with a BESS compared to

that without a BESS. DIgSILENT Power Factory v15.1.7 software simulated the energy and power data to examine the optimal size of the BESS, as shown in Tables 1 and 2.

Table 1. PV size and location in IU29NDN.

	Test System	Node	kVA	kW
PV	IU29NDN	27	25	20

Table 2. BESS size and location in IU29NDN.

	Test System	Node	KAh
BESS	IU29NDN	27	31.9

Peak demand shaving is still possible with storage capacities below about 0.90 MWh per industrial unit, regardless of the installed solar PV capacity. However, when storage capacity exceeds 0.90 MWh per unit, higher PV capacities can lead to even greater reductions in peak demand. This occurs because larger storage allows a significant reduction in evening demand, sometimes shifting peak demand to early in the day, making the impact of solar PV on reducing daytime demand more noticeable.

As PV penetration increases, energy production on the load side may exceed consumer demand. To mitigate this, the BESS charges when PV generation exceeds demand and discharges when demand rises. This advantage can be modeled using the following Equations (10) and (11).

$$P_{Excess} = P_{PV} - P_{Demand} \quad (10)$$

P_{Excess} is the excess power available for storage;
P_{PV} is the power generated power by the PV system;
P_{Demand} is the power demand at load side.

When $P_{Excess} > 0$, the battery charges, and when $P_{Excess} > P_{PV}$, the battery discharges

$$E_{Charge}(t) = \eta_{Ch} \times \min(P_{Excess}(t), \frac{E_{max} - E(t)}{\Delta t}) \quad (11)$$

E_{Charge} represents the amount of energy stored in the battery;
E_{max} represents the maximum storage capacity of the BESS;
$E(t)$ represents the current energy stored in the battery at a time *t*

The higher the efficiency results, the lesser the energy loss during battery charging. Reducing energy loss is crucial for optimizing the overall system performance and storing more generated energy. Minimizing energy losses, reducing grid stress, and maximizing financial returns by charging during low-cost periods and discharging during peak demand collectively optimize a PV system's performance and economic viability with an integrated BESS [36].

Proposed Model Predictive Control

The MPC technique reduces peak PV energy and load demand periods while optimizing battery consumption. MPC guarantees maximum efficiency and flexibility by re-optimizing power flow at each control interval by regularly updating its predictions based on real-time system data. This MPC approach for the proposed system (shown in Figure 2) improves PV sharing and load sharing capacity, which may both be significantly increased without depending on outside signals from the grid operator.

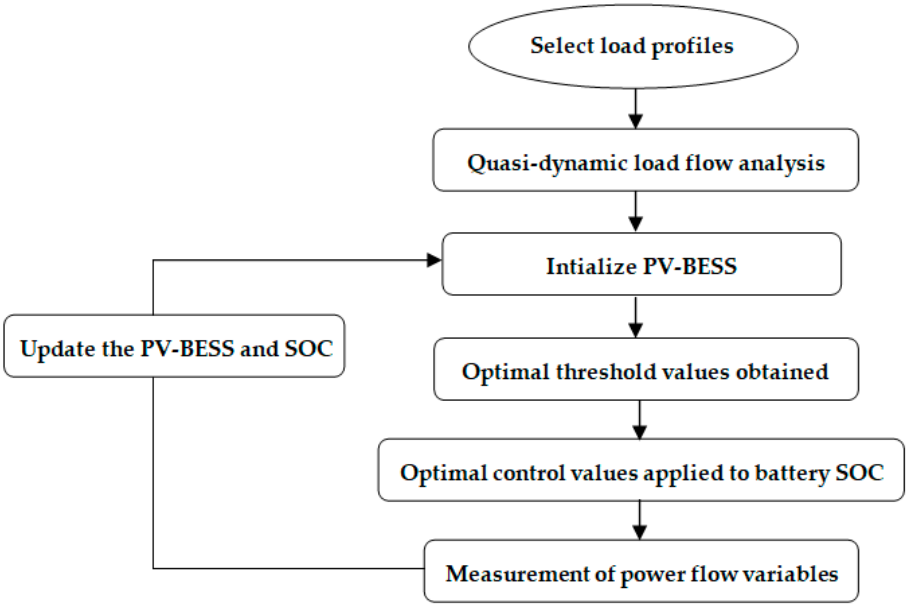

Figure 2. Proposed model predictive control.

The optimum control problem is handled using initial battery SOC measurements, load profiles, and anticipated PV data. Model predictive control controls the output production of each model, including PV systems with storage batteries, by anticipating future output values based on previous data and trends [37,38]. This work introduces a distinctive optimum control problem formulation for achieving peak shaving targets while maintaining efficient energy management and grid stability.

3. The Objective Functions of Peak Shaving in IU29NDN

The rising cost of electricity for utility companies and consumers is driven by high peak demand. The most promising option for peak shaving involves connecting BESSs to the distribution network. This approach can be implemented in residential structures, industries, and grids to achieve peak shaving. Peak shaving is achieved by charging BESSs during low-demand periods (off-peak) and discharging them during high-demand periods.

3.1. Cost Objective Function

The proposed model aims to maximize economic benefits, reduce high power imports during peak hours and demand, lower electricity costs, and enhance the use of BESS. Equations (12)–(15) present the objective functions of cost analysis and peak shaving analysis with state-of-charge constraints.

$$\mathrm{Cost_{total}} = \sum_{t=1}^{T} \left(\mathrm{Cost_{energy}}(t) + \mathrm{Cost_{BESS}}(t) + \mathrm{Cost_{maintenance}}(t)\right) \quad (12)$$

$$\mathrm{P_{load}}(t) = \mathrm{P_{grid}}(t) + \mathrm{P_{BESS}}(t) \quad (13)$$

where $\mathrm{P_{load}}\ (t)$ is the power demand at time t;

$\mathrm{P_{Grid}}\ (t)$ is the power supplied by the grid at time t;

$\mathrm{P_{BESS}}(t)$ is the power supplied or absorbed by the BESS at time t.

3.2. Peak Shaving Objective Function

The following term helps in reducing the peak power drawn from the grid.

$$\text{Minimize} \sum_{t=1}^{T} P_{grid}(t)^2 \tag{14}$$

It is subjected to the constraint

$$SOC_{min} \leq SOC(t) \leq SOC_{max} \tag{15}$$

The peak load shaving program consists of BESS-optimized control. The specifics are provided in the following subsections. The single line practical distribution network model shown in Figure 3 includes a fundamental distribution system. The model consists of electric transformers. Transformer1 contains two buses: 110 kV on the high side and 11 kV on the low side. The transformer is four units in size, with a power rating of 20 MVA. The secondary winding is star-connected, and neutral-grounded, whereas the primary winding is delta-connected.

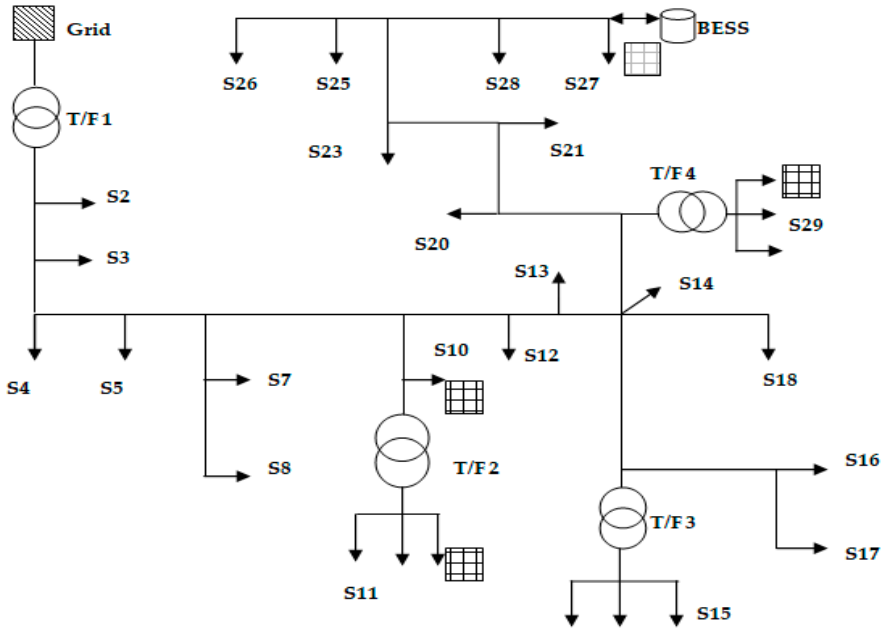

Figure 3. Single-line diagram of an IU29NDN model for the smart grid of Puducherry in India.

PV facilities have been available at a few feeders. The distribution model and network simulation software used the DIgSILENT Power Factory application to examine the load profile. The DIgSILENT Power Factory simulation model of the IU29NDN is shown in Appendix A.

4. Experimental Procedure for Peak Shaving on IU29NDN

Quasi-dynamic load flow analysis (QLFA) for three different seasons (summer, monsoon, and winter) was performed on the IU29NDN [39]. A solar PV-BESS was added to node 27 of the IU29NDN, which is powered by a three-phase overhead wire from a 110 kV substation. Different load profiles were chosen for the 27 nodes in the network. The data were divided into two groups to highlight the factors influencing the incorporation of PV-BESS systems.

(i) The performance settings for distinct nodes, such as voltage and active power of different feeds.
(ii) The feeder's performance and variations for the specified performance criteria, such as peak load shaving with and without a BESS.

Simulations of the distribution load flow have been conducted.

4.1. Load Data for IU29NDN

The 12-month measurement period for IU29NDN load demand is from 7 June 2022 to 31 May 2023. Every minute, a sample of the raw data is taken and averaged over a 15-min period. Figures 4–6 illustrate a load profile for the week from 7 June 2022 to 13 June 2022.

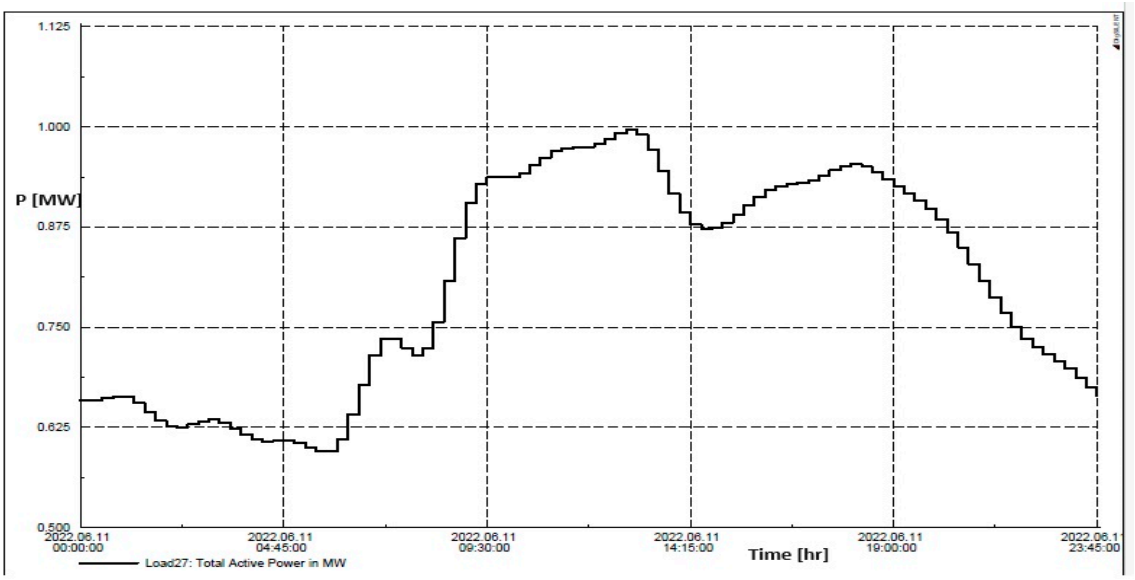

Figure 4. Electricity load profile of IU29NDN in summer season.

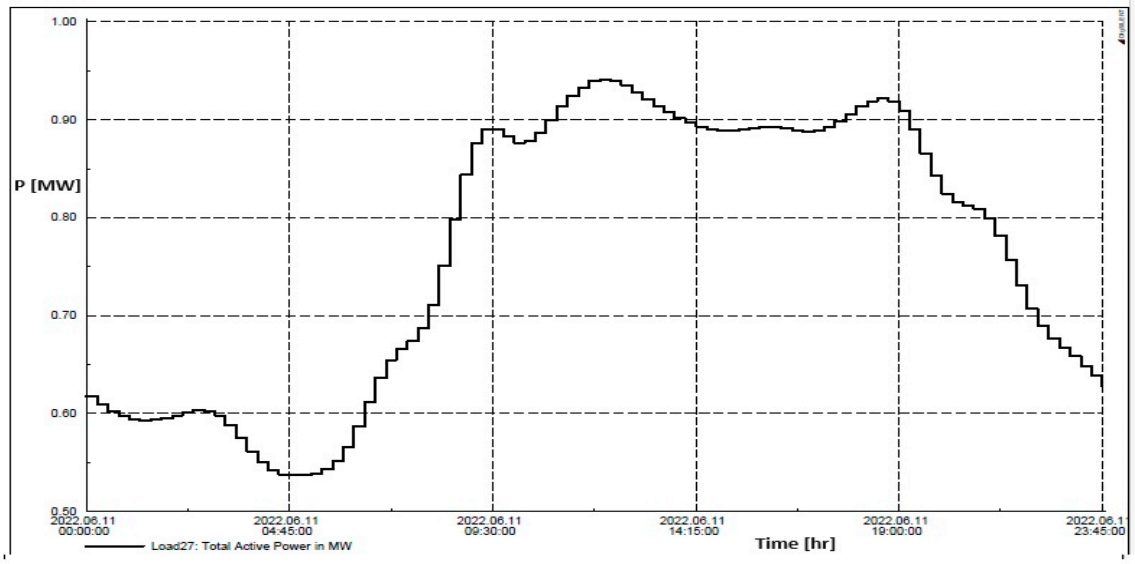

Figure 5. Electricity load profile of IU29NDN in monsoon season.

There is about 77 kW of peak demand on average. Figure 7 provides an example of a load profile averaged over one week. Furthermore, the amount of power used increases around 8:00 a.m. and decreases at 9:00 p.m.

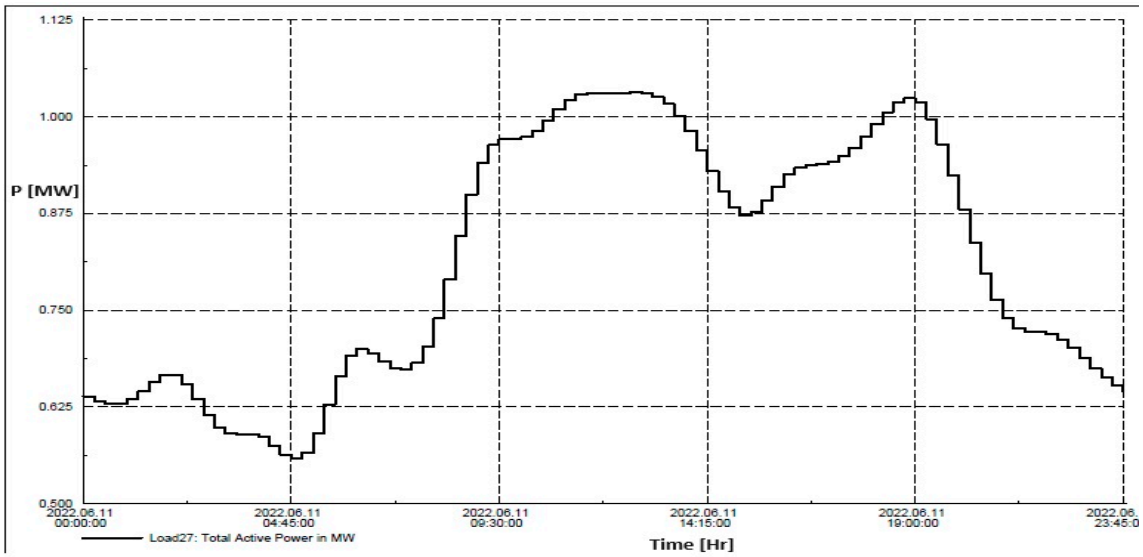

Figure 6. Electricity load profile of IU29NDN in winter season.

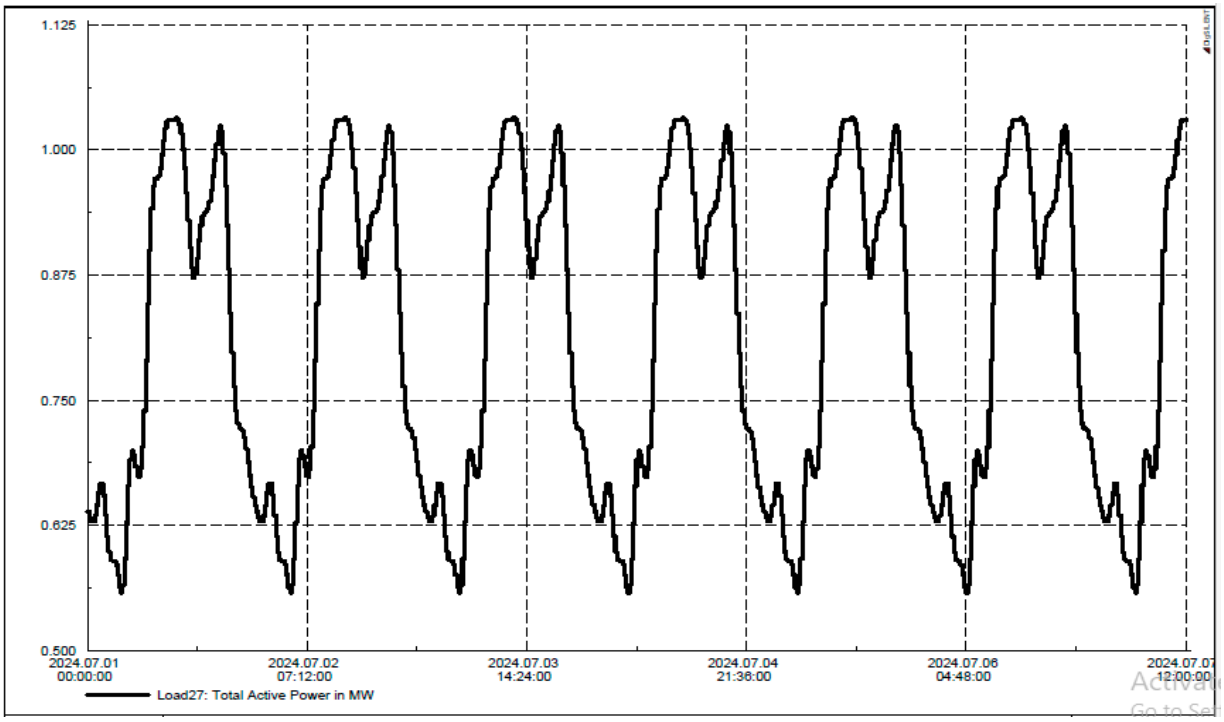

Figure 7. One-week averaged load profile of IU29NDN.

4.2. BESS-Optimized Control

The battery's power rating P_{Rated} and usable energy E_{Usable} are specified as 0.3 MW and 0.25 kWh, respectively. These values are determined under minimal voltage limits by the optimal control of the BESS at a SOC of 20%. Figure 8 illustrates the possibility of minimizing the workings of the BESS according to battery ratings. The peak load region is increased; ΔP_L shows the lowered peak load power, while P_O and E_O, respectively, represent the output power and output energy of the BESS.

Initially, the optimal control system seeks to decrease the peak load power by utilizing all the battery available energy, as illustrated in Figure 8. Next, the power rating or P_{Rated} is looked at and the BESS is restricted by its energy rating if $P_O \leq P_{Rated}$. The complete available energy is utilized, and the drop in peak load power (ΔP_L) equals output

power $P_O(\Delta P_L = P_O)$. However, if the BESS output power is beyond the rated capacity ($P_O > P_{Rated}$), the discharge power is limited to the rated value $P_O = P_{Rated}$.

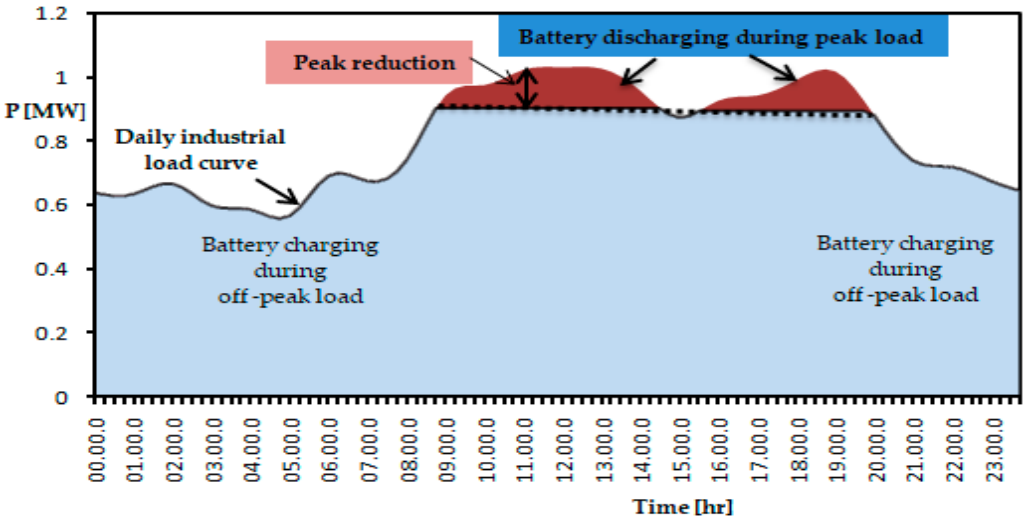

Figure 8. Expanded peak load regions and discharge-power curves for BESS control.

Therefore, peak load shaving power (ΔP_L) is restricted to its power rating $\Delta P_L = P_O = P_{Rated}$. With respect to these energy and power limitations, a BESS has the capacity to produce a perfect discharge-power profile P_{Dis} (t).

4.3. PV Control

The control strategies and the proposed management ensure that the average power from the BESS and the instantaneous power from the PV work as per the SOC of the battery. The PV generation during charging mode should generate extra power to store up to SOC, which comes to 80%. On the other hand, when the SOC drops to 20% in the discharge mode of the battery, the PV should generate power. Additionally, when there is more PV generation or low demand such that $P_O > 0$, the BESS can charge until it reaches the limit (80%). When there is less power generation from PV, the grid provides the power required by the BESS, even in high demand ($P_O < 0$), assuring assistance progression up to the lower limit of SOC. Therefore, the load power (P_L) control is being assured by the related PV-BESS as per the flowchart given in Figure 9.

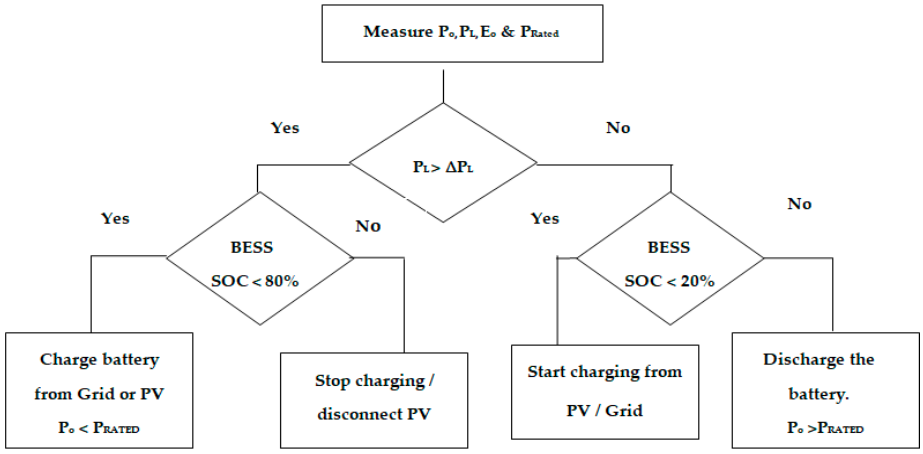

Figure 9. Flow chart of PV-BESS for control and determination.

The optimal discharge profile, $P_{Dis}(t)$, corresponds to the portion of the load profile that is supplied by the BESS between the start of discharge at t = t_{dis} and the end of discharge at t = t_{Stop}. The profile of the BESS is shown in Figure 10.

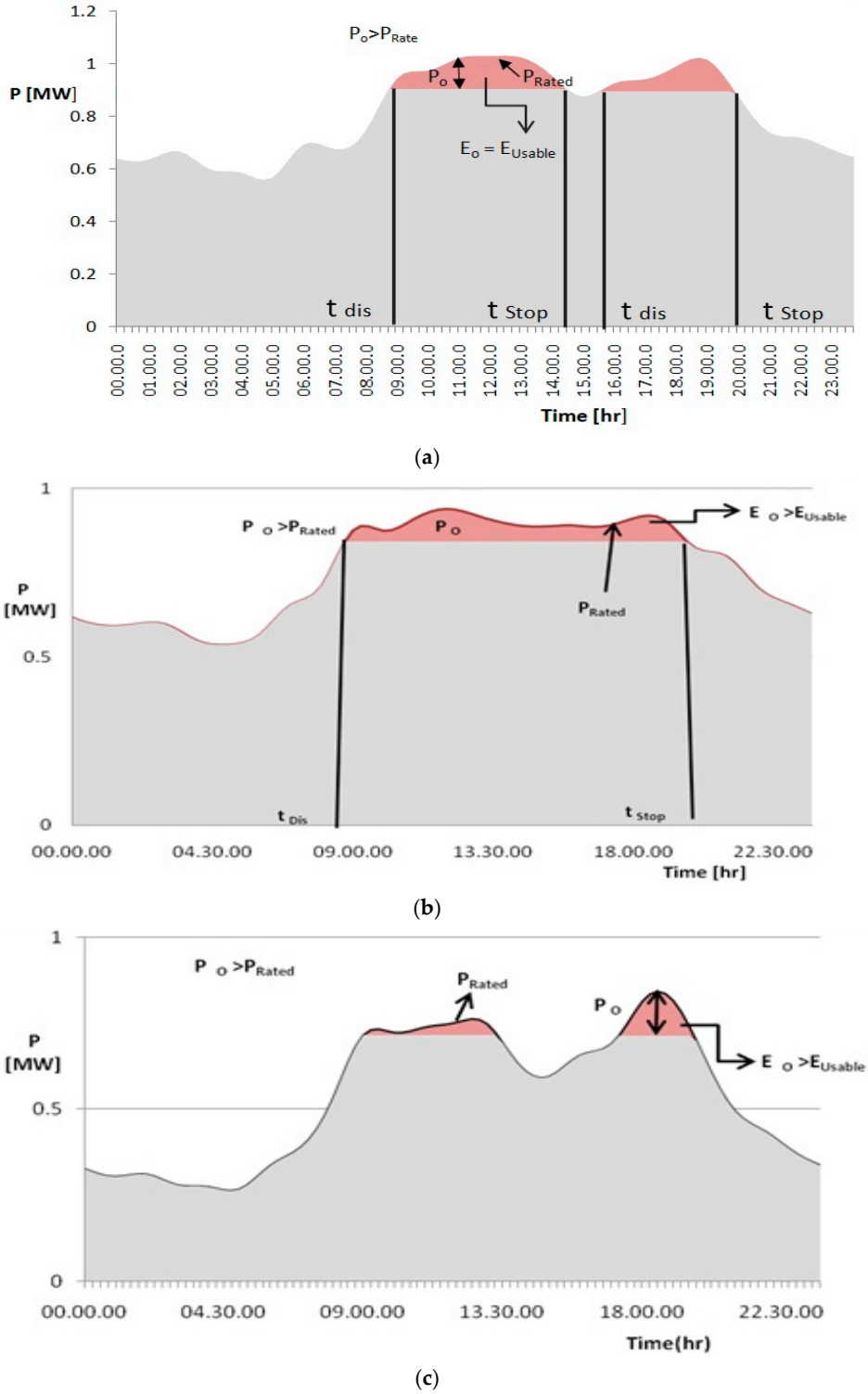

Figure 10. Limitation of BESS by the battery available energy for (**a**) summer, (**b**) monsoon, and (**c**) winter.

4.4. Peak Shaving Strategy

Figure 11 gathers additional peak load shaving studies. Table 3 explains the peak demand time for three seasons. Table 4 presents the outcome of the peak load shaving operation. Additionally, the table illustrates the maximum demand simulations.

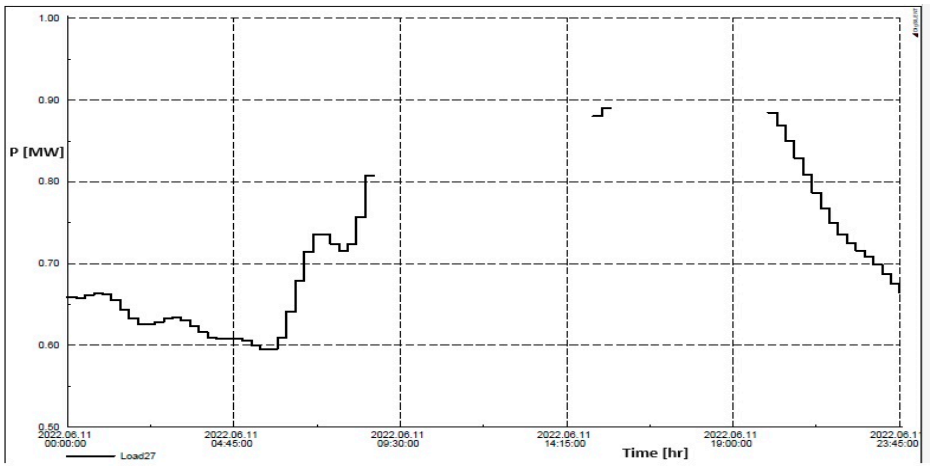

(**a**)

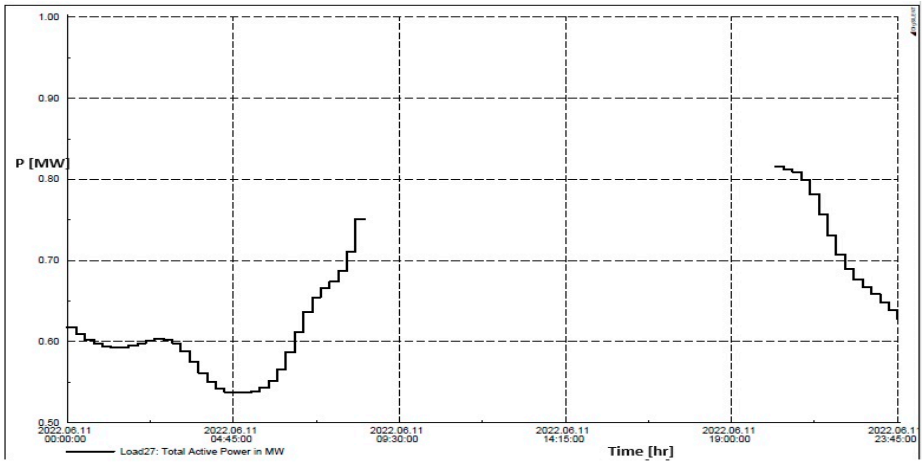

(**b**)

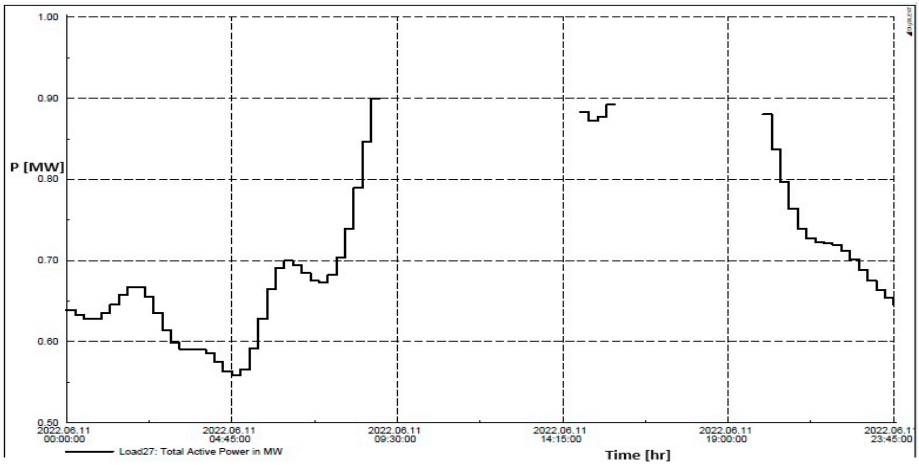

(**c**)

Figure 11. Numerous experimental results of peak load shaving during (**a**) summer, (**b**) monsoon, and (**c**) winter seasons.

Table 3. Peak demand time for various seasons.

Season	Moment of Peak Demand	
	Starting Time	Ending Time
Summer	11:15 a.m. 05:30 p.m.	01:15 p.m. 07:00 p.m.
Monsoon	11:15 a.m. 05:15 p.m.	01:00 p.m. 07:30 p.m.
Winter	11:00 a.m. 05:15 p.m.	01:45 p.m. 07:00 p.m.

Table 4. Peak demand and expected demand reduction.

Interval	Peak Demand (MW)	Expected Peak Reduction (MW)	Battery Scheduling Power (MWh)
Summer (March–June)	0.85	0.21	0.11
Monsoon (July–October)	0.927	0.11	0.224
Winter (November–February)	0.91	0.035	0.1

The monsoon season (July to October) presents a challenging high-peak scenario for peak shaving applications, as continuous peaks occur over an extended period. In contrast, the period from March to June offers an ideal scenario where peak shaving can effectively reduce sharp peak loads, resulting in a significant 20% reduction in peak demand. Table 4 shows peak demand and expected demand reduction, with SOC for all trials from summer to winter exceeding the 20% minimum demand.

The changing effect of the delivered power is evident from the plots of Figure 12a–c presenting the battery power and SOC profiles for the peak load shaving during the day. The battery is completely charged during off-peak hours and is ready for discharge during peak hours. About 35.9 MW, 23.32 MW, and 22.8 MW peak demand is deducted from the original peak load during the summer, monsoon, and winter seasons. Discharging time increases throughout the summer and decreases during the monsoon. This indicates that the power rating of the battery P_{Rated} limits the BESS. Moreover, an additional peak load reduction was calculated from the actual load profile, yielding two important findings. Economic analysis has demonstrated the financial feasibility of adopting BESSs for peak shaving in industrial loads (discussed in Section 4.5). Additionally, the performance of the peak shaving scheme is measured by the peak load error margin, which is alternately indicated by the results.

4.5. Economic Benefit of BESSs

A financial assessment is performed based on the scenarios detailed in Tables 5 and 6. The internal rate of return (IRR) is evaluated from an investment perspective, with a 4.3% IRR established as the break-even point benchmark. The primary cost driver is the heterogeneous battery price, which dominates the overall investment expense.

Table 5. Potential savings based on peak reduction.

Interval	Expected Savings from Peak Saving (MW)	Expected Total Savings (INR)
Summer (March–June)	41	INR 1,230,000
Monsoon (July–October)	12	INR 360,000
Winter (November–February)	28	INR 840,000
Total	81	INR 2,430,000

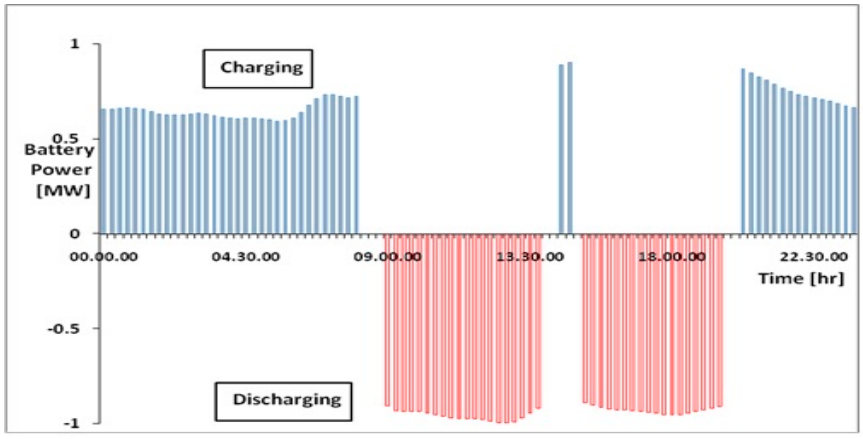

(**a**)

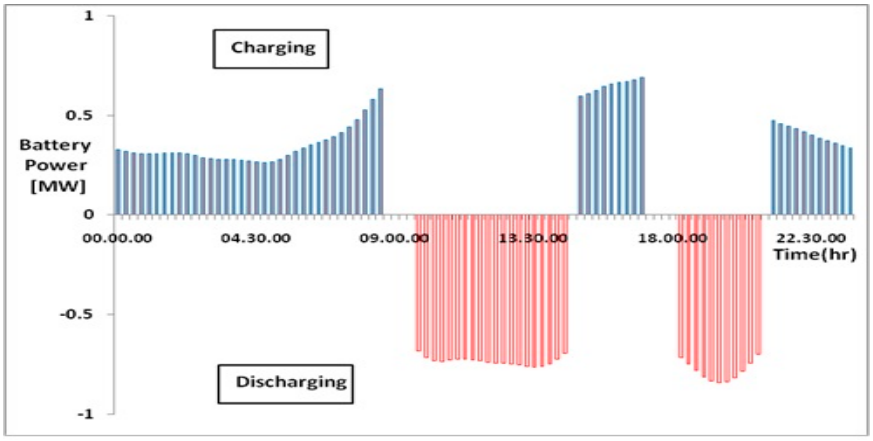

(**b**)

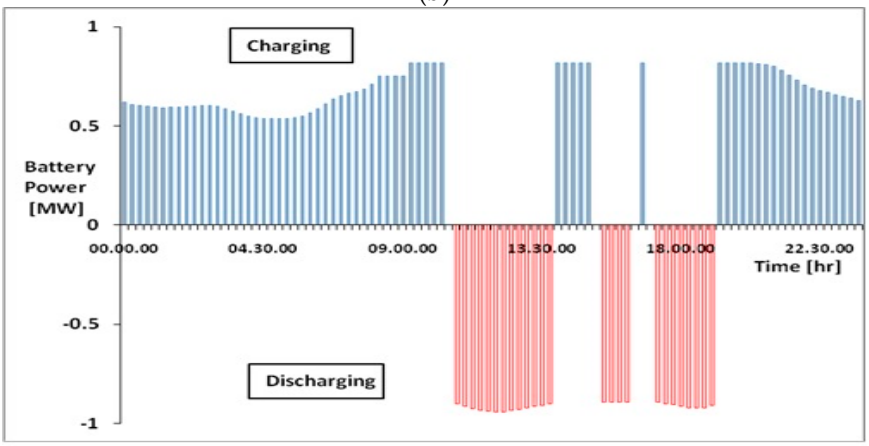

(**c**)

Figure 12. Battery power profiles for (**a**) summer, (**b**) monsoon, and (**c**) winter.

Table 6. Investments of BESSs for peak load shaving application.

Item	Expected Cost
1. Inverter	194,150 INR/50 kw
2. Li Battery	1,008,033 INR/100 kwh
3. Maintenance	9240 INR/Kw

The battery price decreased from 12,000 INR/kWh in 2023 to 9478 INR/kWh in 2025, with an IRR of around 9%, beyond the break-even mark. The research study predicts battery prices will drop below 6710 INR/kWh by 2030, resulting in an IRR of more than

15%. The Puducherry State Electricity Board imposes a demand charge of 6.12 INR/kW for connections above 11 kV, along with a peak load penalty of 50 INR/kW. In the calculation of IRR, two scenarios are the base, one Demand charge 35 INR/kW, and the second peak load deduction is 41 MW in the summer.

5. Conclusions

This study examined the use of time-series and quasi-dynamic LFA in the proposed practical Puducherry smart grid IU29NDN for industrial loads with seasonal variations. The proposed quasi-dynamic LFA enables effective integration of PV-BESS in the distribution network. Simulations are performed to compute the power flow at the 27 nodes of the practical IU29NDN test system with a 24-h time horizon, having a 15-min step size to attain higher accuracy.

In order to lower peak demands, PV-BESS systems were installed at the Puducherry smart grid system in which peak shaving and energy losses over three seasons are two challenging technical goals that were achieved by the integrated functioning of PV-BESS and demonstrated by the simulation results at node 27.

The results of the proposed work with integrated PV-BESS reduce peak power consumption and energy losses. This study demonstrates the effectiveness of optimizing BESSs for peak shaving and financial viability. By adopting an MPC-based algorithm design framework with infinite horizon planning and one-step optimization, the control strategy can efficiently satisfy various constraints inherent in the controlled plants, thereby achieving optimal peak shaving performance and reducing energy costs. Implementing proper battery scheduling and Model predictive control technology, the system reduces annual peak demand by 80 MW. This optimization also effectively reduces peak loads, mitigating energy and power constraints despite seasonal variations.

The research reveals key findings, including BESS ability to customize discharge power profiles to meet energy demands. Additionally, peak load shaving power is optimized within rated capacity limits, and battery power and SOC profiles accurately calculate peak demand deductions. This results in an impressive 86.03 MW annual reduction. Moreover, energy consumption is also optimized in this case, which leads to improvement in potential saving. This research presented the calculation of load demand for three seasons in IU29NDN and an average peak demand for one week. SOC helps control the BESS to minimize working and limit voltage. The use of BESSs for managing peak load in certain regions is explained. The optimal discharge profile gives the limitations of discharge capacity for the three seasons of peak demand reduction compared and tabulated. In the summer, reducing the peak demand profile is more effective.

A comprehensive financial assessment is also conducted, calculating the internal rate of return to evaluate the investment's viability and potential returns. Integrating BESS and MPC technology optimizes peak shaving, reduces energy constraints, and ensures financial viability, making it an attractive solution for renewable energy applications. The evolution of investment and rate of returns by installing PV-BESS is discussed and tabulated. The economic benefits of implementing PV-BESS in the IU29NDN system are discussed, focusing on investment recovery, maintenance cost savings, and peak load electricity cost reduction.

Author Contributions: Methodology, M.A.S.B.; Software, M.A.S.B.; Validation, M.S.; Formal analysis, M.S.; Investigation, M.S. and S.D.; Writing—original draft, M.A.S.B.; Writing—review & editing, M.S., S.D. and M.E.; Visualization, M.E.; Supervision, M.S. and S.D. All authors have read and agreed to the published version of the manuscript.

Funding: This research received no external funding.

Data Availability Statement: The data are not publicly available, as the authors do not have permission to share them due to privacy concerns.

Acknowledgments: The authors express their gratitude to the authority of Puducherry Technological University in Puducherry 605015, India, for providing the resources required to complete this work.

Conflicts of Interest: The authors declare no conflict of interest.

Abbreviations

Acronyms	
BESS	Battery energy storage system
PV	Photovoltaic system
MPC	Model predictive control
IU29NDN	Indian Utility 29 Node Distribution Network
DER	Distributed energy resource
BMS	Battery management system
B-SDPVG	Battery-Sourced Distributed Photovoltaic Generation
NPV	Net present value
DNO	Distribution network operator
DSM	Demand-side management
SOC	State of charge
DOD	Depth of discharge
SMP	System marginal price
QLFA	Quasi-dynamic load flow analysis
IRR	Internal rate of return
INR	Indian rupee
Parameters	
$\eta_{\mathrm{RTP}}(\alpha)$	Round-trip efficiency
η_{ch}	Charging efficiency
η_{Dis}	Discharging efficiency
P_{nom}	Power rating of the converter
SOC_{Min}	Minimum permitted states of charge
SOC_{Max}	Maximum permitted states of charge
C_{req}	Battery minimum or required capacity
T_l	Deterioration time
P_{Excess}	The excess power available for storage
P_{PV}	The power generated power by PV system
P_{Demand}	The power demand at load side
E_{Charge}	The amount of energy stored in a battery
$E_{\max}$	The maximum storage capacity of a BESS
Indices	
t	index of time
h	index of hour
Variables	
$P_{BESS}(t)$	The power supplied or absorbed by the BESS at time t
$P_{Ch}(t)$	Charging power at a time t
$P_{Dis}(t)$	Discharging power at a time t
$SOC(t)$	State of charge at a time t
Δt	Time step duration at a time t
$C_{\delta}(t)$	Battery maximum capacity at a time t
$P_{Excess}(t)$	The excess power available for storage at a time t
$E(t)$	The current energy stored in the battery at a time t
$P_{load}\ (t)$	The power demand at time t
$P_{Grid}(t)$	The power supplied by the grid at time t

Appendix A

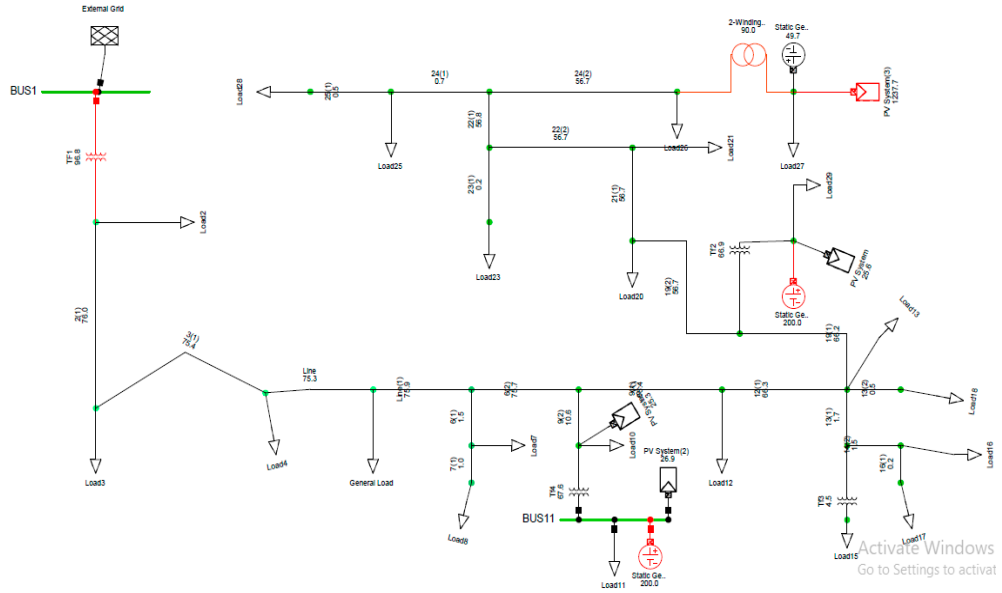

Figure A1. Simulation Diagram of the IU29NDN Modeled in DIgSILENT Power Factory v15.1.7.

References

1. Albertini, R.; Yabe, V.T.; Di Santo, S.G. Distributed Energy Resources Management Systems (DERMS). In *Green Energy and Technology*; Springer International Publishing: Berlin/Heidelberg, Germany, 2023; pp. 143–172. [CrossRef]
2. Eskandari, M.; Rajabi, A.; Savkin, A.V.; Moradi, M.H.; Dong, Z.Y. Battery energy storage systems (BESSs) and the economy-dynamics of microgrids: Review, analysis, and classification for standardization of BESSs applications. *J. Energy Storage* **2022**, *55*, 105627. [CrossRef]
3. Stanelyte, D.; Radziukyniene, N.; Radziukynas, V. Overview of Demand-Response Services: A Review. *Energies* **2022**, *15*, 1659. [CrossRef]
4. Gevorgian, V.; Koralewicz, P.; Shah, S.; Mendiola, E.; Wallen, R.; Pico, H.V. *Photovoltaic Plant and Battery Energy Storage System Integration at NREL's Flatirons Campus*; OSTI OAI (U.S. Department of Energy Office of Scientific and Technical Information): Oak Ridge, TN, USA, 2022. [CrossRef]
5. Duman, C.; Erden, H.S.; Gönül, Ö.; Güler, Ö. Optimal sizing of PV-BESS units for home energy management system-equipped households considering day-ahead load scheduling for demand response and self-consumption. *Energy Build.* **2022**, *267*, 112164. [CrossRef]
6. Thokar, R.A.; Gupta, N.; Niazi, K.R.; Swarnkar, A.; Meena, N.K. Multiobjective nested optimization framework for simultaneous integration of multiple photovoltaic and battery energy storage systems in distribution networks. *J. Energy Storage* **2021**, *35*, 102263. [CrossRef]
7. Pham, T.D. Integration of Photovoltaic Units, Wind Turbine Units, Battery Energy Storage System, and Capacitor Bank in the Distribution System for Minimizing Total Costs Considering Harmonic Distortions. *Iran. J. Sci. Technol. Trans. Electr. Eng.* **2023**, *47*, 1265–1282. [CrossRef]
8. Yuan, Z.; Wang, W.; Wang, H.; Yildizbasi, A. Developed Coyote Optimization Algorithm and its application to optimal parameters estimation of PEMFC model. *Energy Rep.* **2020**, *6*, 1106–1117. [CrossRef]
9. Chaduvula, H.; Das, D. Investigating effect of various time varying load models in grid connected microgrid system integrated with renewables and cogeneration units. *Int. J. Ambient. Energy* **2023**, *44*, 2540–2552. [CrossRef]
10. Kumtepeli, V.; Zhao, Y.; Naumann, M.; Tripathi, A.; Wang, Y.; Jossen, A.; Hesse, H. Design and analysis of an aging-aware energy management system for islanded grids using mixed-integer quadratic programming. *Int. J. Energy Res.* **2019**, *43*, 4127–4147. [CrossRef]
11. K, S.; N, S.; Suriyan, K.; R, N.; Venusamy, K. Impacts of residential energy storage system modeling on power system. *Sustain. Environ.* **2022**, *8*, 2125905. [CrossRef]
12. Tsai, C.-T.; Cheng, Y.-S.; Lin, K.-H.; Chen, C.-L. Effects of a Battery Energy Storage System on the Operating Schedule of a Renewable Energy-Based Time-of-Use Rate Industrial User under the Demand Bidding Mechanism of Taipower. *Sustainability* **2021**, *13*, 3576. [CrossRef]

13. Saini, P.; Gidwani, L. An investigation for battery energy storage system installation with renewable energy resources in distribution system by considering residential, commercial and industrial load models. *J. Energy Storage* **2021**, *45*, 103493. [CrossRef]
14. Yang, B.; Guo, Y.; Xiao, X.; Tian, P. Bi-level Capacity Planning of Wind-PV-Battery Hybrid Generation System Considering Return on Investment. *Energies* **2020**, *13*, 3046. [CrossRef]
15. Tahir, M.J.; Rasheed, M.B.; Rahmat, M.K. Optimal Placement of Capacitors in Radial Distribution Grids via Enhanced Modified Particle Swarm Optimization. *Energies* **2022**, *15*, 2452. [CrossRef]
16. Zheng, M.; Meinrenken, C.J.; Lackner, K.S. Smart households: Dispatch strategies and economic analysis of distributed energy storage for residential peak shaving. *Appl. Energy* **2015**, *147*, 246–257. [CrossRef]
17. Gelleschus, R.; Böttiger, M.; Bocklisch, T. Optimization-Based Control Concept with Feed-in and Demand Peak Shaving for a PV Battery Heat Pump Heat Storage System. *Energies* **2019**, *12*, 2098. [CrossRef]
18. Decentralized Cloud-Based Approaches for Cross-Sector Demand Side Management-ProQuest. Proquest.com. 2021. Available online: https://www.proquest.com/openview/cb0841a03e987d0a1d9fe0d72cd0c8f0/1?pq-origsite=gscholar&cbl=2026366&diss=y (accessed on 30 December 2024).
19. Liu, J.; Wang, H.; Du, Y.; Lu, Y.; Wang, Z. Multi-objective optimal peak load shaving strategy using coordinated scheduling of EVs and BESS with adoption of MORBHPSO. *J. Energy Storage* **2023**, *64*, 107121. [CrossRef]
20. Rana, M.; Romlie, M.F.; Abdullah, M.F.; Uddin, M.; Sarkar, M.R. A novel peak load shaving algorithm for isolated microgrid using hybrid PV-BESS system. *Energy* **2021**, *234*, 121157. [CrossRef]
21. Zhu, J.; Cui, X.; Ni, W. Model predictive control based control strategy for battery energy storage system integrated power plant meeting deep load peak shaving demand. *J. Energy Storage* **2021**, *46*, 103811. [CrossRef]
22. Yang, H.; Sun, Z.; Dou, X.; Li, L.; Yu, J.; Huo, X.; Pang, C. Optimal Scheduling and Compensation Pricing Method for Load Aggregators Based on Limited Peak Shaving Budget and Time Segment Value. *Energies* **2024**, *17*, 5759. [CrossRef]
23. Kanwhen, O.; Mohamed, A. Energy storage systems for commercial buildings in dense urban regions: NYC case study. *Energy Rep.* **2023**, *10*, 300–318. [CrossRef]
24. Almutairi, Z.A.; Eltamaly, A.M. Synergistic Effects of Energy Storage Systems and Demand-Side Management in Optimizing Zero-Carbon Smart Grid Systems. *Energies* **2024**, *17*, 5637. [CrossRef]
25. Efkarpidis, N.A.; Imoscopi, S.; Geidl, M.; Cini, A.; Lukovic, S.; Alippi, C.; Herbst, I. Peak shaving in distribution networks using stationary energy storage systems: A Swiss case study. *Sustain. Energy Grids Netw.* **2023**, *34*, 101018. [CrossRef]
26. Ren, Z.; Li, H.; Yan, W.; Lv, W.; Zhang, G.; Lv, L.; Sun, L.; Sun, Z.; Gao, W. Comprehensive evaluation on production and recycling of lithium-ion batteries: A critical review. *Renew. Sustain. Energy Rev.* **2023**, *185*, 113585. [CrossRef]
27. Jiang, X.; Jin, Y.; Zheng, X.; Hu, G.; Zeng, Q. Optimal configuration of grid-side battery energy storage system under power marketization. *Appl. Energy* **2020**, *272*, 115242. [CrossRef]
28. Ma, M.; Huang, H.; Song, X.; Peña-Mora, F.; Zhang, Z.; Chen, J. Optimal sizing and operations of shared energy storage systems in distribution networks: A bi-level programming approach. *Appl. Energy* **2022**, *307*, 118170. [CrossRef]
29. Mahdavi, E.; Asadpour, S.; Macedo, L.H.; Romero, R. Reconfiguration of Distribution Networks with Simultaneous Allocation of Distributed Generation Using the Whale Optimization Algorithm. *Energies* **2023**, *16*, 4560. [CrossRef]
30. Ratshitanga, M.; Ayeleso, A.; Krishnamurthy, S.; Rose, G.; Moussavou, A.A.A.; Adonis, M. Battery Storage Use in the Value Chain of Power Systems. *Energies* **2024**, *17*, 921. [CrossRef]
31. Tiemann, P.H.; Bensmann, A.; Stuke, V.; Hanke-Rauschenbach, R. Electrical energy storage for industrial grid fee reduction–A large scale analysis. *Energy Convers. Manag.* **2020**, *208*, 112539. [CrossRef]
32. Mostafa, M.H.; Aleem, S.H.E.A.; Ali, S.G.; Ali, Z.M.; Abdelaziz, A.Y. Techno-economic assessment of energy storage systems using annualized life cycle cost of storage (LCCOS) and levelized cost of energy (LCOE) metrics. *J. Energy Storage* **2020**, *29*, 101345. [CrossRef]
33. Zdiri, M.A.; Guesmi, T.; Alshammari, B.M.; Alqunun, K.; Almalaq, A.; Ben Salem, F.; Abdallah, H.H.; Toumi, A. Design and Analysis of Sliding-Mode Artificial Neural Network Control Strategy for Hybrid PV-Battery-Supercapacitor System. *Energies* **2022**, *15*, 4099. [CrossRef]
34. Bereczki, B.; Hartmann, B.; Kertész, S. Industrial Application of Battery Energy Storage Systems: Peak shaving. In Proceedings of the 2019 7th International Youth Conference on Energy (IYCE), Bled, Slovenia, 3–6 July 2019. [CrossRef]
35. Cossutta, M.; Pholboon, S.; McKechnie, J.; Sumner, M. Techno-economic and environmental analysis of community energy management for peak shaving. *Energy Convers. Manag.* **2022**, *251*, 114900. [CrossRef]
36. Su, X.; Sun, B.; Wang, J.; Ruan, H.; Zhang, W.; Bao, Y. Experimental study on charging energy efficiency of lithium-ion battery under different charging stress. *J. Energy Storage* **2023**, *68*, 107793. [CrossRef]
37. Liu, D.; Zhang, H.; Liang, X.; Deng, S. Model Predictive Control for Three-Phase, Four-Leg Dynamic Voltage Restorer. *Energies* **2024**, *17*, 5622. [CrossRef]

38. Prakash, R.; Dheer, D. An Integrated Approach for Yaw Stability of Linear Time Varying Bicycle Model Utilizing Adaptive Model Predictive Control. *Jordan J. Electr. Eng.* **2023**, *9*, 566–590. [CrossRef]
39. Sasi Bhushan, M.A.; Sudhakaran, M. Time-series quasi-dynamic load flow analysis with seasonal load variation to resolve energy nexus for a practical distribution network in Puducherry smart grid system incorporating harmonic analysis and mitigation. *Energy Nexus* **2023**, *11*, 100234. [CrossRef]